Received: 22 June 2020 | Revised: 10 August 2020 | Accepted: 18 August 2020

DOI: 10.1111/ina.12735

ORIGINAL ARTICLE

WILEY

Three-dimensional analysis of the effect of human movement on indoor airflow patterns

Arup Bhattacharya[1] | Jovan Pantelic[2] | Ali Ghahramani[2,3] | Ehsan S. Mousavi[1,2]

[1]Department of Construction Science and Management, Clemson University, Clemson, SC, USA

[2]Center for the Built Environment, University of California, Berkeley, CA, USA

[3]Department of Building, School of Design and Environment, National University of Singapore, Singapore City, Singapore

Correspondence
Ehsan Mousavi, Department of Construction Science and Management, Clemson University, 2-132 Lee Hall, Clemson, SC, 29634, USA.
Email: mousavi@clemson.edu

Funding information
Directorate for Engineering, Grant/Award Number: 2012827

Abstract

Human activity is known to leave significant effects on indoor airflow patterns. These patterns are carefully designed for many facilities such as cleanrooms, pharmaceutical settings, and healthcare environments, where human-induced wakes contribute to the transport of contaminants. Therefore, the knowledge about these wakes as it relates to indoor air quality is critical. As a result, a series of experiments were conducted in a controlled chamber to study the three-dimensional effects of true human walking on airflow. Experiments were designed to capture the effect of human walking under three different flow conditions, and for two different walking schemes. The results show that the effect of walking on the airflow is not negligible and can sustain up to 10 seconds after the moving body has passed. Walking on a straight line creates significant change in the velocity normal to the walking path and vertical to the plane of walking movement. These changes were detectable till 1.0 m away from the walking track. Also, the similarity between airflow patterns of walking once and twice illustrated a promising opportunity of predicting the flow patterns of random walk from a set of base cases.

KEYWORDS

3-D velocities, human movement, human-induced contamination, indoor airflow, infectious disease control, ultrasound sensor

1 | INTRODUCTION

Concerns regarding the indoor air quality are of great importance to the scientific community as indoor air is the most dominant exposure to human.[1] On average, 90% of our total time is spent indoors and a large portion of indoor contaminants lives and moves via air.[2] Indoor air quality takes a variety of meanings in different buildings. There are controlled environments such as healthcare facilities, cleanrooms, and laboratories that must follow stringent guidelines not only to maintain air quality in a generic fashion, but to create airflow patterns to remove/contain/divert contaminants. In cleanrooms, maintaining the prescribed degree of cleanliness is very important as contaminants that are transported by airflow can deposit onto the surfaces of the semiconductor products, affecting the reliability and quality of the final product. Pharmaceutical industries must ensure air cleanliness during manufacturing of sterile drugs,[3] while research laboratories must avoid contamination especially when conducting experiments on organisms, quality control, or microfluidic devices.[4] Healthcare facilities are one of the most concerned sectors regarding air cleanliness as a system malfunction can result in adverse patient outcomes.[5] The recent COVID-19 outbreak has drawn remarkable attention to the effect of airflow pattern on the dispersion of pathogenic agents within the hospital. Not only the safety of patients, but the health of healthcare personnel is at stake during an outbreak.[6] Hence, indoor air quality goes far beyond thermal comfort in such sensitive premises. While the above-mentioned spaces have different characteristics and are designed by different codes, they share

Journal Name INA
Manuscript No. 12735
WILEY
No. of pages: 15 Dispatch: 5-9-2020
PE: Balakumar C. CE: Kasthuri S

one common trait; airflow patterns must be designed such that the concentration of unwanted substances in the space is minimized.

Many particles are capable to stay afloat for a long time as they follow airstreams.[7] Thus, in order to understand airborne particle dispersion in the space, it is important that airflow movement patterns are fully understood.[8,9] In practice, these airstreams are controlled by (de)pressurizing the space with respect to its adjoining spaces and/or the location of air inlets and outlets.[10-12] For example, operating rooms maintain a positive pressure to achieve a net outward flow, and the air outlets should be placed at the floor level on the surrounding walls.[13,14] Still, studies have shown that surgical site infections occur despite the positive pressure in the operating room.[15,16] The knowledge about air movement patterns and factors that alter these patterns is essential for a thorough understanding of contamination transport indoors.

A series of epidemiological studies dating back to 40 years have identified factors such as door motion and movements of individual and other physical movements such as movement of the patient bed and accessories and medical equipment, to have significant impacts on disease spread.[17-21] In one of the earlier studies, Josephson and colleagues (1988) found that placing the patient room near the nursing unit raised the probability of airborne transmission of nosocomial varicella due to increased activity at the nursing station, suggesting that human movement has a real effect on the spread of airborne contaminants.[18] Leclair et al(1980) also predicted that moving traffic of human subjects indoor have an effect on particle transmission.[22] Shih et al (2007) numerically simulated the airflow dynamics inside an isolation room to demonstrate that moving person and movement of doors affect air distribution, including velocity and pressure fields.[23] Hang et al (2015) studied potential transmission of airborne infectious diseases through CFD and validated the findings by experiments.[24] This study showed that the sweeping effects of door motion, together with the ventilated airflow are responsible for volumetric exchange of contaminated air across the door, even in the presence of a differential pressure. Several other researchers have studied the velocity field created by moving objects in various settings.[25-27]

More recently and with the advancements in the computer technology, experiments and computer simulations were conducted to understand the airflow characteristics under the influence of moving human body and supply air from above in an airliner cabin. A study conducted in an airline cabin demonstrated that the wakes generated by the human movement interacted with the flow field and affected the distribution of contaminant concentration.[28] Luo et al (2018) conducted experiments in a small-scale chamber followed by computational fluid dynamics (CFD) simulations showing that the moving body contributed to a downward flow carrying the contaminants toward the floor and dispersing them to surrounding areas.[29] The rate of this dispersion was shown to depend on the speed of the occupant. Another numerical simulation of contaminant distribution in a hospital inpatient ward indicated that contaminants are carried in the wakes generated by moving objects (eg, people, equipment).[30] Brohus et al (2006) numerically simulated a laminar airflow orthopedic surgery room to establish that the local field as well as the entire room airflow was substantially influenced by the movements and continuous periodic walks were found to generate complex turbulent flow inside the room, decreasing the ventilation efficiency.[31]

Practical Implications

This work characterizes the effect of human movement on airflow patterns under various initial conditions scenarios. We utilized novel three-dimensional indoor air velocity sensors, and the measure changes in air velocity as a result of human walk. Results showed that velocities increase up to six times the background values in the still air (<0.1 m/s average velocity). This change could sustain up to 15 seconds before returning to background, and it was observed in all three dimensions. There seems to be a need to include the human movement component in airflow calculations, especially in premises where controlling airborne aerosols is critical (eg, hospitals, cleanrooms).

The aerodynamic effects of a moving object in airflow patterns and contaminant transport have been widely studied in settings other than healthcare as well.[32] Human movement induce wakes in the indoor airflow and consequently leads to contaminant dispersion.[33] Rouaud and team (2004) studied the external perturbations in the air flow fields using a small-scale model filled with water citing that conducting experiments in full-scale buildings were difficult.[34] Cheng and Lin (2016) investigated the interaction between the airflow and the human movement under stratum ventilation using manikins to substitute human body and found that moving bodies create blockage effect.[35] Matsumoto and Ohba (2004) evaluated the effectiveness of displacement ventilation under moving objects. The results demonstrated that the movement speed and modes of movement—parallel and perpendicular to the inlet air, significantly impacted the distribution of temperature and the ventilation effectiveness.[36] Choi and the team (2012) studied contaminant transport by human motions in a setting where two rooms (one contaminated and one clean) were connected by a vestibule. Through large-eddy simulations, they found that motion-induced wakes aided in the increase of compartment-to-compartment contaminant transport.[37] Han et al (2014) conducted a numerical analysis of an in-flight infection by airborne disease using a Eularian-Lagrangian approach, and the infection risk was modeled using likelihood analysis.[38] The results supported previous studies that human movement disturbs the air distribution and airflow motion in the airliner cabin. This paper also demonstrated that human movement prevented aerosols from traveling across the aisle of the airplane. Human walk enhanced the air-mixing, increasing the probability of transport of aerosols along the moving path. Tao et al (2017) suggested that walking significantly impacted the distribution of particles by changing the airflow momentum. They also showed that even after the walk was over, the

wakes continued to alter the flow field over time.[39] Bhattacharya et al (2020) conducted a series of experiments in an actual cleanroom to determine effects of moving traffic in cross-contamination, and their results proved that the direction of the movements has significant impact in changing the airflow pattern.[40] Saidi et al (2011) numerically simulated airflow inside a cleanroom to study the effects of contaminant source motion in spread of the contaminants.[41] They showed that the dispersion of contaminants greatly depends on the motion of the sources, and contamination spread can be controlled if the movement is in the dominant direction of the airflow. Hang et al (2014) studied the flow disturbances resulting from the walk of a healthcare worker with swinging arms and legs in an isolation room using CFD simulation.[42] The results demonstrated a complex mixing process, different from simulating the simplified human walk (eg, without considering the swinging motion of legs and hands). It also showed that the wakes generated from these walks could be more than 6 meters long and these fields can take 30 - 60 seconds after the movement was stopped to get back to the initial condition. These studies clearly suggest that the movement of human being has significant potential impacts on the flow fields in a ventilated enclosure.

Most of the published studies have been concentrating on examining the flow fields near the moving body and the temporal flow profiles, despite a number of qualitative, experimental, and numerical studies on investigating the impacts a moving body on the flow fields, very little was found on experimental measurements during the actual human walk. To address that, this study is conducted to understand the transient pattern of airflow characteristics under the influence of a moving human subject. The spatial-temporal flow fields generated from the walking movement was also studied. What truly sets this work apart from the existing literature is the use of a new ultrasound technique to measure the three-dimensional indoor air velocities, verified by another set of omnidirectional airspeed sensors. We study the effect of human walking on indoor airflow patterns under three different initial conditions and for two different walking schemes.

2 | METHODOLOGY

2.1 | Chamber Geometry

In summer 2019, the controlled environment chamber in UC Berkeley's Center for Built Environment was available to conduct tests. This sealed chamber was a research facility with capabilities to have air supply at various flow rates from wall mounted grille or from ceiling mounted diffusers or from raised floor supply grilles. The chamber was 5.48 × 5.44 × 2.5 m, with a door of 1.98 × 0.98 m at one corner. For the experiments, air was supplied through the 0.3 × 0.3 m grille in at a height of 0.3 m from the ceiling (Figure 1). Excess air was exfiltrated from the chamber mainly through the gaps around the door, creating a positive pressure when the supply fans were on.

2.2 | Test setup and procedure

In order to study effects of the walking movement of a person on the temporal and spatial characteristics of indoor airflow, a series of walking experiments were conducted in the chamber. To eliminate the randomness associated with walk, a 3.04 m long and 0.3 m wide track was defined, and sensors were placed at each side along the track to measure air velocity. The starting point of the walk was 1.1m from the wall across the supply grille and 2.25 m from wall with hinged door (Figure 1B). The measurement units were mounted on tripods and were placed in six rows along imaginary lines perpendicular to the walking track, each located at distance of 0.61 m from the adjacent row, as shown in Figure 1B. The first row was colinear

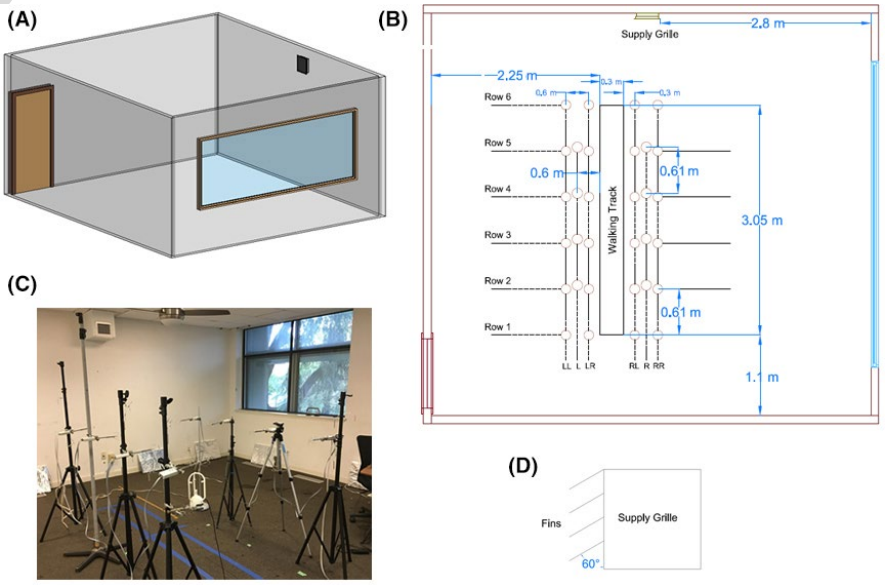

FIGURE 1 Chamber Geometry and Experimental Design

with the start of the track with a pair of sensors on each side of the track, and row 6 was located at 3.05m (10 ft) apart from the first row, colinear with the end of the track and had sensors arranged exactly like that of row 1. The intersection of the vertical and horizontal dimension lines delineated the name of the sensor. For example, sensor L4 is located at the intersection of "L" and "Row 4." The walking track was drawn in such a way that the sensing stations on the right side of the track were directly exposed to the inlet airflow from the supply grille, as evident from Figure 1B and C. Furthermore, the adjustable fins of the supply grille were oriented at 60^0 angle with the vertical plane (Figure 1D) in order to direct the airflow toward the sensing stations.

2.3 | Walking exercise and initial conditions

The experiments were conducted under different initial conditions regarding the inlet airflow from the supply diffuser. Depending on the amount of air supplied to the chamber, there were three separate flow regimes as described below.

a. Still air—during this scenario, the initial steady-state condition inside the experiment chamber was quiescent as the fan and the AHU responsible for air supply to the chamber were not operating, and the supply diffuser was shut off.
b. 70% fan—for the second type of flow regime, the supply fan and the AHU were throttled to operate at 70% of full capacity. The supply grille configuration was as described in Figure 1D. After steady-state condition was reached inside the chamber, the manometer reading indicated a positive pressure differential of 22.4 Pa between the room and outside.
c. 100% fan—for this inlet condition, the supply fan and AHU operated in full capacity and the orientation of the supply grille was the same as case b. With 190 cfm (90 L/s)[43] air inlet during this flow setting, the positive differential pressure between the chamber and outside was measured to be 37.3 Pa at steady state.

Two walking scenarios were defined. For walking once, the person began the walking movement from the start point and covered the track distance (3.04m)up to 3 seconds before coming to a standstill (walking speed = 1.02 m/s). During this movement, the movement direction of the individual walking was toward the supply grille—designated as forward movement. During walking twice and similar to walking once, the person walked in the forward direction facing the inlet for three seconds until the entire track distance was covered, stopped walking, and remained stationary at the end of the track for 1 second and moved backward for 3 seconds to reach the start point and stop walking. The walking exercises in these experiments were realistic, where the arms and legs were swinging naturally. But the airflow data due to swinging motion through the gaps around arm and feet were not collected, and the walking exercise was considered to be simplified. As the human walk had inherent randomness, the walking durations were recorded using handheld stopwatch. The durations for all the experiments were recorded and averaged, which are provided in the Table 1, with the standard deviations presented in parenthesis. For these two walking exercises under the above described flow regimes, different test case scenarios were defined, and multiple repetition was performed for each of them in order to increase number of observations at each location and to ascertain statistical consistency of the collected data (Table 1).

2.4 | Sensing instruments

During the experiments, two types of sensors were used to measure the air velocity—omnidirectional and ultrasound. The omnidirectional sensors recorded only the velocity magnitude, whereas the ultrasound sensors logged air velocity components in three Cartesian coordinates, where x-axis was the principle direction of human movement, y-axis was perpendicular to the track, and z-axis was normal to the plane of walking track. The ultrasound sensors were placed such a way that the probe of this sensors is at the nearest proximity to that of the omnidirectional.

The omnidirectional velocity sensing system employed was AirDistSys 5000 manufactured by Sensor Electronic, Poland. These sensors consist of a transducer, a converter, and a transmitter. SensoAnemo5100LSF is a transducer with omnidirectional (spherical) sensor with a diameter of 2mm, measurement speed range of 0.05 to 5 m/s, ±0.02 m/s or ± 1.5% of reading accuracy of measurement, directional sensitivity error for v > 2m/s of ± 2.5% the actual value. Through this sensing system, one data point was logged every two seconds. The sensor, designed for low speed measurement indoors, has wide range of frequency response and high sensitivity.

TABLE 1 Experiment conditions

	Inlet Flow	Walking Exercise	Average walking time	Data Logging Duration	No. of trials
Test 1	Still	Once	3.18 s ($\sigma = 0.27$)	60 s	33
Test 2	70%	Once	3.2 s ($\sigma = 0.13$)	60 s	33
Test 3	100%	Once	3.09 s ($\sigma = 0.17$)	60 s	33
Test 4	Still	Twice	7.18 s ($\sigma = 0.23$)	60 s	33
Test 5	70%	Twice	7.01 s ($\sigma = 0.18$)	60 s	33
Test 6	100%	Twice	7.07 s ($\sigma = 0.14$)	60 s	33

The transducer measures instantaneous mean airspeed and standard deviation of airspeed. The probes in all the sensors are connected to SensoDACon series 5400 converter which allows to convert a digital signal with Sensoanemo transducer to the analog signal of velocity as output which is recorded in the system through wireless connection using SensoBee transmitter and receiver.

The ultrasound sensing system, utilized to log 4 data points of 3-dimensional air velocity components per second, was developed indigenously at the Center for the Built Environment in University of California, Berkeley. At the heart of this lightweight and portable sensor, there is a CH-101 ultrasonic transceivers, utilizing new microelectromechanical systems technology for ultrasonic range finding.[44] A tetrahedral arrangement of four such transceivers, minimum required number to capture 3-D flow, was used that provided enhanced measurement redundancy. These transceivers communicate with the outside world through a carrier board—a four-layer printed circuit board. The firmware used to control the microprocessor, which can be optimized for each application at run-time, also enables shielding errors generated by the wakes from anemometer support struts. The anemometer has a resolution and starting threshold of 0.01 m/s, an absolute airspeed error of 0.05 m/s at a given orientation with minimal filtering, 3.1 ° angle and 0.11 m/s velocity errors over 360 ° azimuthal rotation, and 3.5 ° angle and 0.07 m/s velocity errors over 135 ° vertical declination. For more details, please refer the works by Ghahramani et al (2019) and Arens and colleagues (2020).[45,46] Figure 2 shows a typical ultrasound sensor used in these experiments, with the tetrahedral arrangement of the transceivers.

2.5 | Statistical Analysis

The time-averaged outputs of the omnidirectional sensing system for every test case were collected for 60 seconds which generated 30 data points for each 33 replications. In order to obtain a transient velocity profile, all 30 data points collected over the repeated experiments were averaged, for all the sensing stations. The results indicated consistency in the collected data at each point in time, for every measuring stations. To assess the consistency of measurements, all the spatial-temporal data points were combined in one array (**V**). The relative standard errors (RSEs) were defined as the data standard error (SE) of **V** its average. Since the RSEs were normalized be average velocity, it was reasonable to present the data in percentage (Table 2). RSE was largest for quiescent air, perhaps due to the low average value of data points.

3 | RESULTS AND DISCUSSIONS

Indoor airflow characteristics were influenced by the induced flow resulted from walking movements of a person. The data collected during different experimental setup were analyzed, and the results are presented specific to the test case scenarios. As stated in the methodology section, air velocities were measured by two different sensors. In this section, measurements for both sensors will be discussed, and the outcomes will be compared. Specifically, the ultrasound sensor enabled measuring air velocity vectors. To our knowledge, this is the first report of three-dimensional velocity measurements of human-induced indoor airflow.

3.1 | Coherence of the anemometer methods

Data from the two sensing techniques were mostly consistent with two major differences: 1) The ultrasound sensors measured four data points per second which resulted in capturing fluctuations in the flow. 2) The omnidirectional sensors tend to show speeds over background for a longer period of time, whereas the ultrasound sensors' reading dropped to (near) zero faster. As far as detecting a lag in data logging, the two techniques performed rather similarly (Table 3). The difference could mainly lie in the roots of different measurement techniques adopted by the sensors. The omnidirectional sensors measure, via a hot wire, the average speed of air in two-second intervals in a small spherical control volume (r = 25 mm). The low resolution of data sensing led to larger magnitudes during a

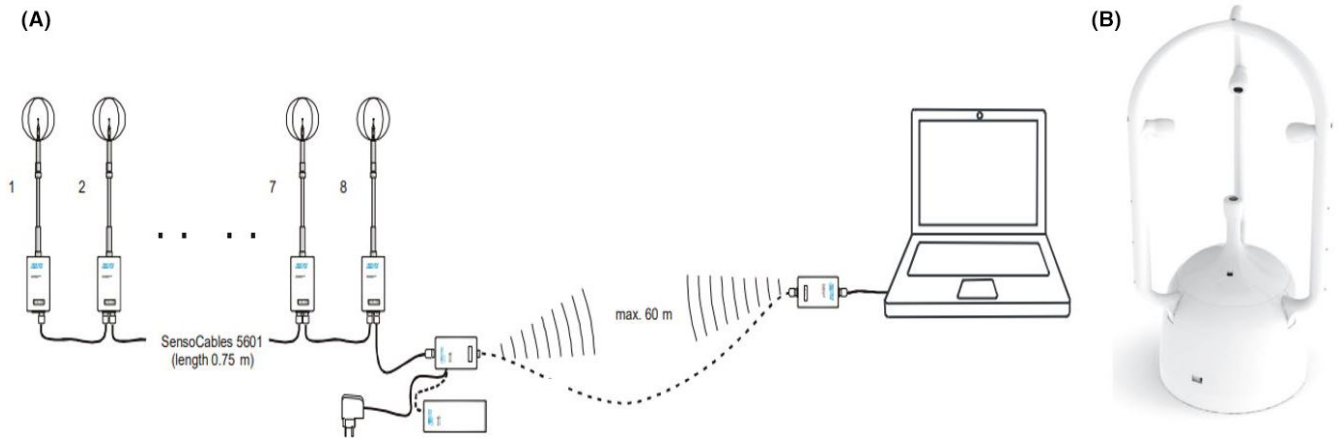

FIGURE 2 Measurement Devices: (A) Omnidirectional courtesy to device catalog and (B) ultrasound

longer time span. However, this technique does not account for temporal fluctuations in airspeed. In a sense, the magnitudes reported by the omnidirectional sensors are the volume-averaged readings by the sensor during the two-second interval. During the same interval, the ultrasound sensors produced 8 data points (4 per second). Nonetheless, the time-average speed of air measured by the two sensing techniques are reasonably consistent. These data points manifested the true fluctuations of air velocity in three dimensions. Later in the paper, we discuss why these fluctuations play an important role in characterizing the true effect of human walk on airflow patterns. In summary, the ultrasound measurement technique led to two novel outcomes, (a) sub-second resolution in data measurements, and (b) indoor air velocity as a 3-D vector quantity.

TABLE 2 Consistency of Data Measurements By Omnidirectional sensors for all Test Repetitions

Experiment	Average RSE
Test 1	13.67%
Test 2	6.90%
Test 3	5.68%
Test 4	19.37%
Test 5	6.92%
Test 6	5.75%

3.2 | Walking once-still air

During experiment setup 1, the initial condition prior to start of movement, the indoor air was quiescent. The data showed that with no other motion than the unidirectional human walk (along the x-axis), there were changes in the air velocity in three dimensions (Table 4). Figure 3 shows the change in velocity magnitude (airspeed) with respect to time. The change in velocity was sensed

TABLE 3 Comparison between the measurements by ultrasound vs. omnidirectional sensors

Sensor	Sensor type	non-zero entries [s]	Peak velocity [m/s]	Lag [s]	Average Velocity [m/s]-(σ)
R2	Omnidirectional	–	0.048	1 s	0.039 (0.028)
	Ultrasound	5 s	0.132	<1 s	0.037 (0.009)
L2	Omnidirectional	–	0.057	1 s	0.043 (0.021)
	Ultrasound	–	0.087	<1 s	0.029 (0.024)
R3	Omnidirectional	16 s	0.079	1 s	0.037 (0.022)
	Ultrasound	7 s	0.103	2 s	0.035 (0.025)
L3	Omnidirectional	16 s	0.099	2 s	0.048 (0.026)
	Ultrasound	10 s	0.110	2 s	0.041 (0.029)
R4	Omnidirectional	16 s	0.151	3 s	0.059 (0.025)
	Ultrasound	10 s	0.132	3 s	0.042 (0.029)
L4	Omnidirectional	16 s	0.168	3 s	0.065 (0.050)
	Ultrasound	13 s	0.214	3 s	0.058 (0.049)
R5	Omnidirectional	15 s	0.160	4 s	0.062 (0.029)
	Ultrasound	11 s	0.104	5 s	0.049 (0.028)
L5	Omnidirectional	15 s	0.194	4 s	0.066 (0.060)
	Ultrasound	15 s	0.174	5 s	0.068 (0.056)

TABLE 4 Three-dimensional velocities, lag, and range of non-zero data recorded by ultrasound sensor

Sensor	Background velocities [m/s]	Maximum Velocity [m/s](time it occurred [s])			
		V	Vx	Vy	Vz
R2	0.0231	0.132 (10.0)	0.119 (11.0)	0.052 (11.0)	0.047 (19.6)
L2	0.0450	0.118 (15.0)	0.051 (10.6)	0.095 (15.0)	0.081 (11.3)
R3	0.0385	0.103 (14.0)	0.057 (12.6)	0.0511 (14.0)	0.057 (20.0)
L3	0.0177	0.089 (14.3)	0.085 (14.3)	0.070 (14.67)	0.026 (16.0)
R4	0.0297	0.113 (13.6)	0.053 (13.6)	0.095 (13.6)	0.043(17.0)
L4	0.0269	0.215 (13)	0.167 (13.0)	0.175 (10.6)	0.081 (13.0)
R5	0.0270	0.115 (15.0)	0.098 (15.0)	0.081 (14.0)	0.039 (14.6)
L5	0.0200	0.180 (15.6)	0.084 (21.3)	0.174 (15.6)	0.081 (17.0)

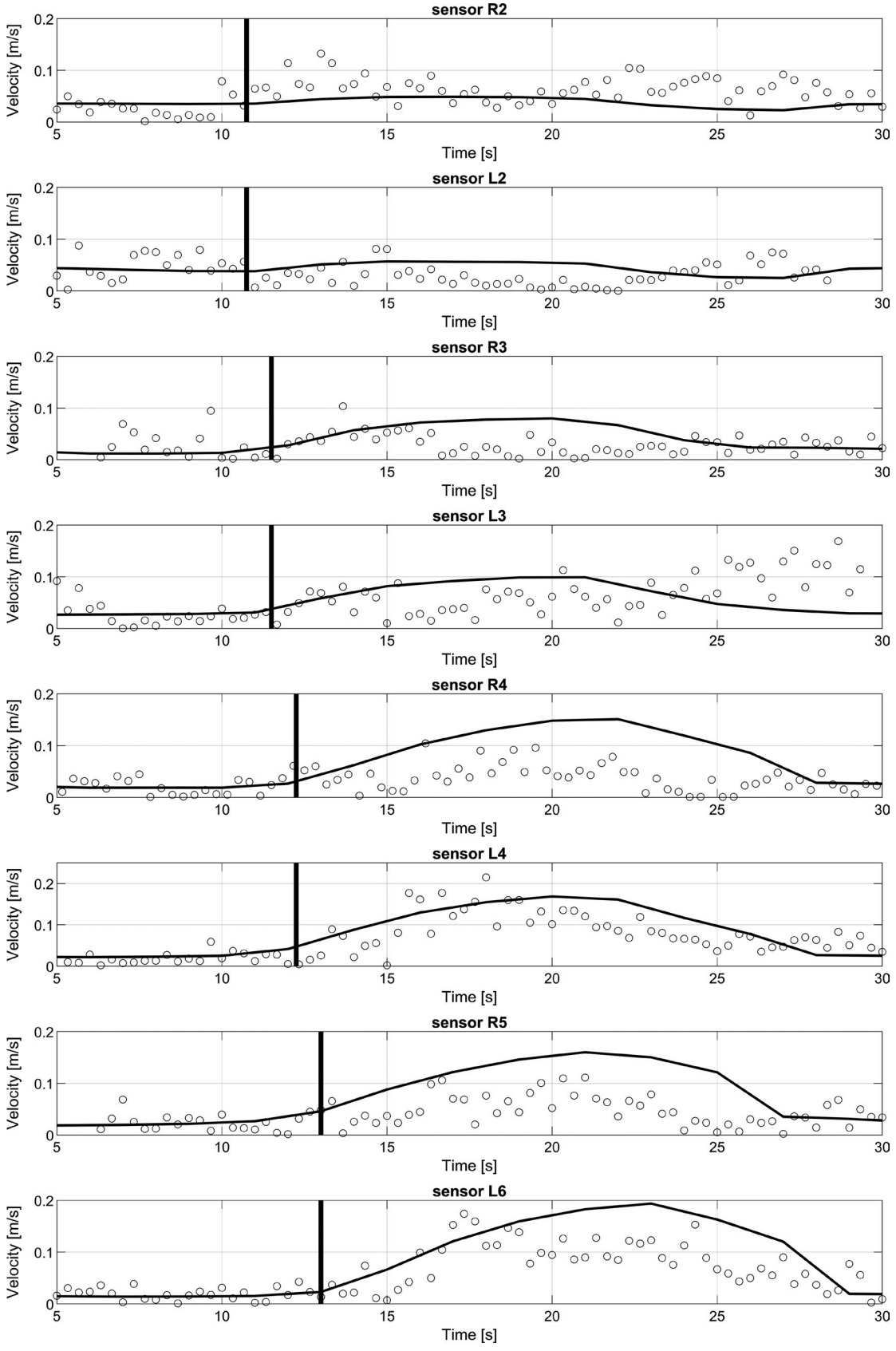

FIGURE 3 Airspeed due to walking once in still air by omnidirectional (-) and ultrasound (°). Vertical lines show the approximate time that the person walked by the sensor

immediately by the onset of walking in sampling stations R2 and L2. After about two seconds, velocities at sampling stations R3 and L3 began to rise. One second later, sensors L4 and R4 showed speeds above zero, and finally, after about five seconds the Row 5 sensors (R5 and L5) sensed the effect of walking on the airflow. Considering three seconds of walking duration, it seemed that the sensors started recording the surge in velocity after the moving body was already past them, resulting the lag between the time the human passed the sensor and the time changes in airflow was recorded. Further, the increase in velocity magnitude over the background values sustained up to 15 seconds. The ultrasound sensors recorded non-zero magnitudes up to about 10 seconds after the walk ended (Figure 3). Both cases reveal that the effect of human walking on the flow is not negligible.

As the movement proceeded, the sensors along the track recorded higher magnitude of velocity than those which were placed before them. For example, sensors R3 and L3 recorded higher magnitude of maximum velocity than R2 and L2, sensors R4 and L4 had higher magnitude of air velocities recorded than the rest. For the first pair of sensors, the air was quiescent before the walk started. As the moving body moved by the sensors, its momentum was transferred to air that increased the velocity of air over background. For the following sensors, the air around was not quiescent anymore and already had some velocities which when interacted with the moving body and had contributed in the higher magnitudes of velocity. Although the moving body made a unidirectional walk along the length of the track (x-axis), the velocity components perpendicular to the track (y-axis) and normal to the plane of the track (z-axis) were recorded (Figure 4).

Results illustrated that none of these components were insignificant. In fact, velocities along the y-axis were in the same order as those along the main direction, indicating that the moving body pushes the air forward and to the sides. The vertical component of velocity (V_z) was not as large as the horizontal components. Nevertheless, the maximum value of V_z was of the same order of magnitude as V_x, and in most cases, the maximum value for V_z did not occur at the same time as the other components were maximum. It must be also noted that all the maximum values of velocity in all three dimensions were between 2 to 10 times larger than the background airspeed. This information, brought by the ultrasound sensing technique, is critical in characterizing indoor airflow patterns. For example, the oscillating behavior of $V_z$is known to be responsible for the resuspension of dust and large particle when they settle on the floor.

3.3 | Air distribution perpendicular to walking direction

The dispersion of human movement-induced airflow fields, perpendicular to the direction of movement, was found to be concentrated near the walking track and velocity dropped quickly with increasing distance from the walking track. Even with varied location of the sensors, that is, data for different rows at different time, exhibited similar trends, with some variations in the magnitude. Figure 5 illustrates the trends in flow field along the width of the test chamber (perpendicular to the walking track) at four different times, measured by omnidirectional sensors located in Row 4, for walking once (bottom graph) and walking twice (top graph). To put this in the context, airspeed measurements were normalized by the background speed (V_{BG}), that is, the average speed of air at each station before the walk began. The dark hatch on the horizontal plane shows (symbolically) the walking track. For walking twice, the velocity magnitude inside the walking track was nearly ~ 6 times V_{BG} and that of walking once was nearly three times V_{BG}. These normalized velocities rapidly approached 1.0 (ie, V_{BG}) for sampling points farther from the walking track. Data showed that the effect of human walking on airflow patterns was only limited to a 1m range [1.85m-2.85m], 0.5m from each side from the center of the walking track. Within the 1.0m range, however, velocities over background were sustained for nearly 15 seconds after the walk ended.

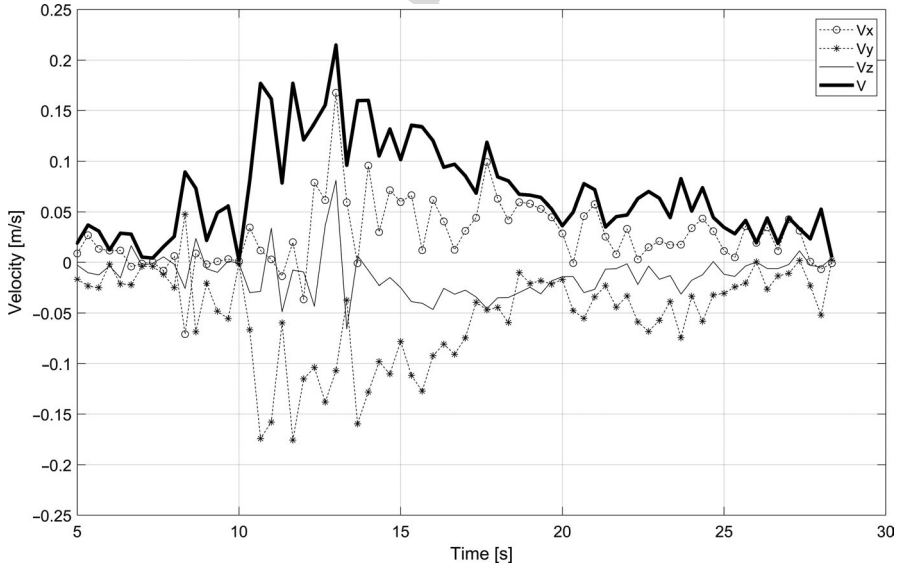

FIGURE 4 Patterns of airspeed for Sensor L3 and the Cartesian components of air velocity

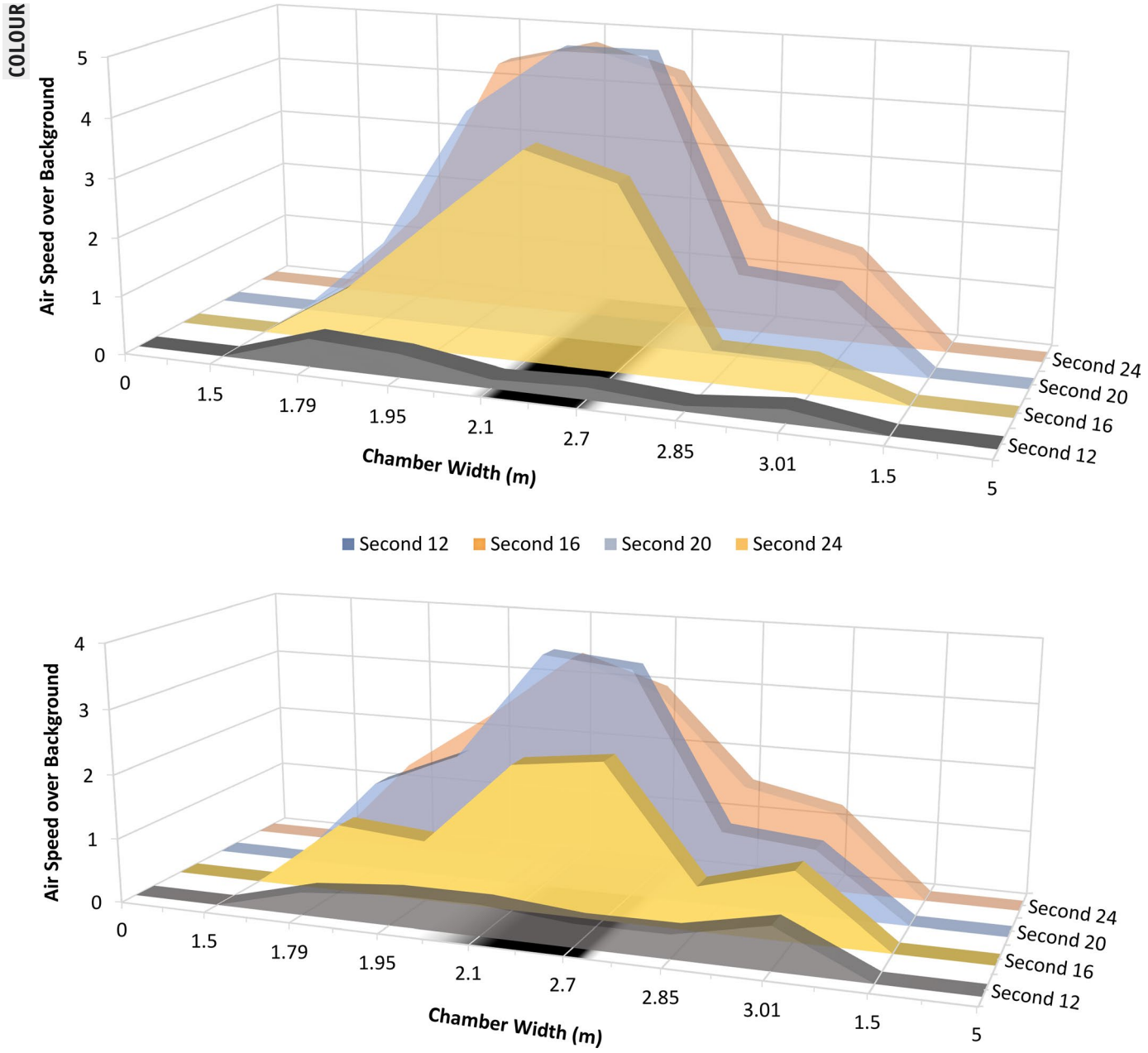

FIGURE 5 Effect of Human Walking on the Airflow Perpendicular to Walking Direction for Walking Once (bottom) and Walking Twice (Top)

3.4 | Walking twice-still air

Even though the movement was present for a longer duration than walking once, the properties associated with characteristics of air movement displayed analogous trends, albeit with higher magnitudes during walking twice. It is demonstrated from Figure 6 that similar to Test 1, all the sensors recorded the beginning of airspeed increase from second 12 apart from sensors R5 and L5 which recorded the beginning of the surge from second 14. The results from walking twice were more interesting as Sensor R4 recorded the highest speed among all the sensors which was 0.26 m/s (~6xV_{BG}) followed by sensor R5 which recorded and 0.24 m/s (~5xV_{BG}), both at second 19. Note that V_{BG} is different for different sampling stations, as it is the time-average velocity of air before the walking began. In the walking twice scenario, the middle sensors recorded high velocities as they virtually experienced the full human walk twice. During the forward movement, the moving body carried the air wakes until the end point, and at this point, the air stream had a motion in the direction of first walk. While moving backward, the initial air was moving in a different direction and the movement of human walk had interacted with the moving air. As a result, one should expect to observe less significant increase in V_x between tests 1 and 4 as the walking direction inverted. Along the Y-axis, however, since walking in both directions led to pushing air to the sides of the walking track, a significant increase in V_y was observed. Worthy to note, the sign of velocity changed for the sensors placed on different sides of the moving body. Table 5 demonstrates the average velocities.

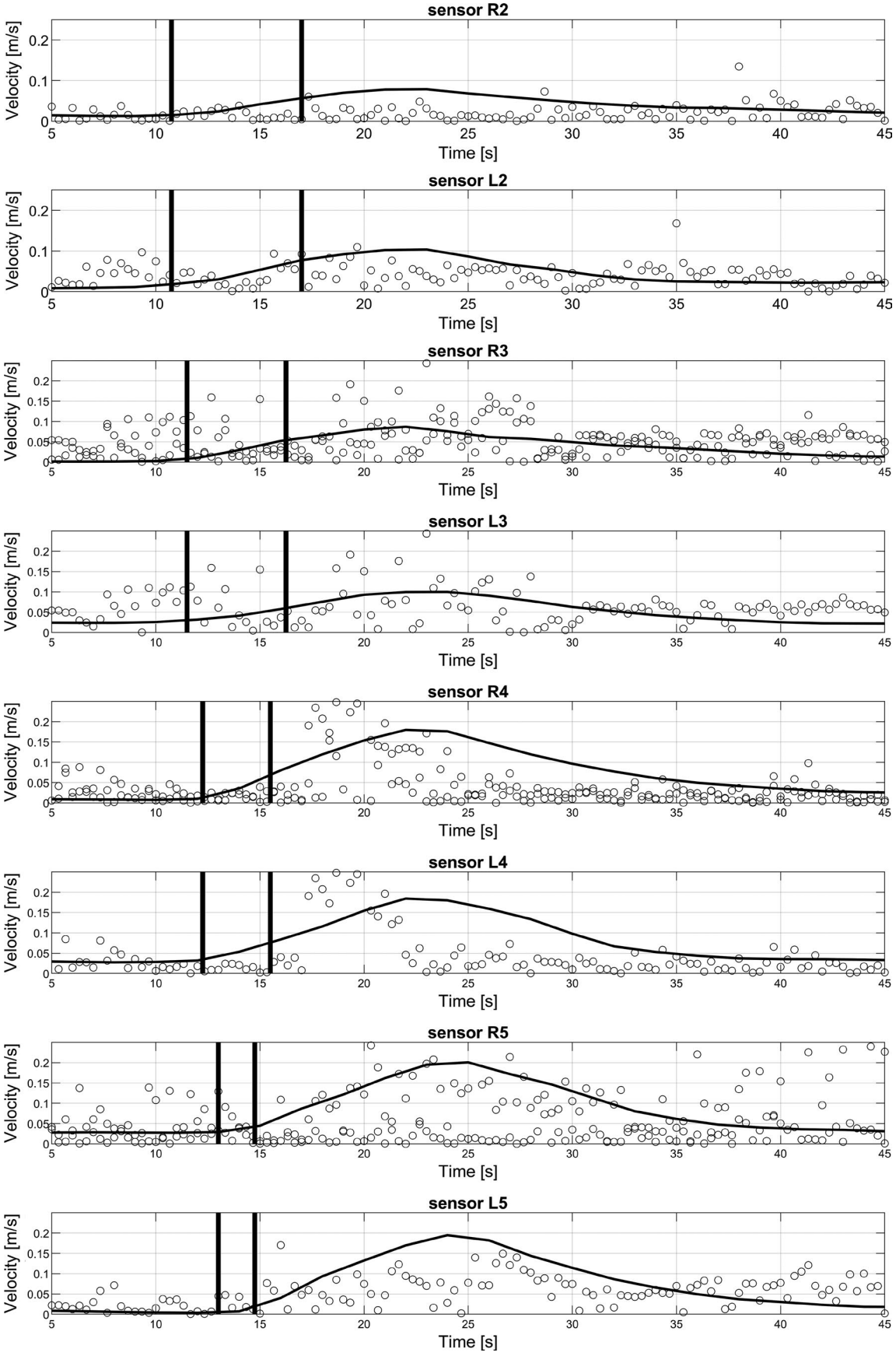

FIGURE 6 Airspeed due to walking twice in still air by omnidirectional (-) and ultrasound (°). Vertical lines show the approximate time that the person walked by the sensor

TABLE 5 Comparison between Time-Averaged Velocity Components of Walking Once and Twice

Sensor	Walking Once			Walking Twice			Velocity Proportions		
	$\frac{\sum_{t=10}^{20} v_x}{N}$	$\frac{\sum_{t=10}^{20} v_y}{N}$	$\frac{\sum_{t=10}^{20} v_z}{N}$	$\frac{\sum_{t=10}^{20} v_x}{N}$	$\frac{\sum_{t=10}^{20} v_y}{N}$	$\frac{\sum_{t=10}^{20} v_z}{N}$	X-axis	Y-axis	Z-axis
Column	A	B	C	D	E	F	(D/A)	(E/B)	(F/D)
R2	0.054	−0.023	−0.018	0.032	−0.036	0.015	0.59	1.57	0.83
L2	0.010	0.017	0.006	0.017	0.096	0.020	1.69	5.72	3.12
R3	0.004	−0.004	−0.003	0.006	−0.009	0.002	1.65	2.00	0.52
L3	0.034	0.024	−0.010	0.018	0.050	−0.016	0.53	2.10	1.60
R4	0.013	−0.036	−0.002	0.021	−0.021	−0.002	1.61	0.59	0.91
L4	0.044	0.083	−0.020	0.014	0.017	−0.014	0.32	0.20	0.71
R5	0.038	−0.019	0.008	0.048	−0.050	−0.010	1.25	2.67	1.21
L5	0.023	0.013	−0.005	−0.006	0.070	−0.002	0.26	5.40	0.42

On average, the x and z components of velocity did not change for the two cases, while the y-component doubled for walking twice.

3.5 | The effect of Initial conditions

In the experimental setup, the airstream was directed in such a way that the sensors in the right side of the walking track (R's) were directly influenced by the inlet air, whereas the sensors in the left side of the track (L's) were free from such direct influence. Obviously, the sensors to which the supply airstream was directed recorded higher magnitudes of velocity. The sensors away from direct exposure to the supply air stream recorded velocity due to walk and the magnitudes are comparable to that of walking in still air. Figure 7 shows one example of such an observation for sensor L4. Especially for walking once, velocity magnitudes are comparable and show very similar behavior. However, since air has an initial velocity prior to the walk, the initial measurements ($t < 10s$) are appreciably higher compared to the still air. Generally, the cases with non-zero initial velocities depicted higher fluctuations, indicating higher potential for turbulence. Nonetheless, the effect of walking was well captured by the sensors (Figure 7). Conversely, those sensors directly exposed to the supply air showed different behaviors with respect to the initial conditions (Figure 8). Most notably, the effect of body movement seemed to be dissolved in the current flow of air. There are minor indications of the walk but not as conspicuous as the other cases.

For each sensor location, the kinetic energy of air is proportional to the sum of Cartesian velocity components, raised to the second power (Eq.1). Further, one can define the time-average initial kinetic energy (K_0) and the time-average walk kinetic energy (K_w) in the following manner:

$$K = \int mv.dv = \frac{1}{2}mv^2 \propto v_x^2 + v_y^2 + v_z^2 \quad (1)$$

$$K_0 = \frac{\int_0^{t=10s} v_x^2 + v_y^2 + v_z^2}{(10-0)} \quad (2)$$

$$K_w = \frac{\int_{10}^{t=20s} v_x^2 + v_y^2 + v_z^2}{(20-10)} \quad (3)$$

These embodiments of kinetic energy can help to compare the sheer effect of walking on the airflow. Table 6 shows the sum of K_0 and K_w recorded in every sensor, and for all the experiment settings. Admittedly, the initial kinetic energy of air considerably rises with the increase in the supply rate. Interestingly, however, the walking period consistently had a higher kinetic energy relative to the background energy (Figure 9). Moreover, the increase ratio in the kinetic energy of air between the two walking cases was between 1.5 to 1.6 times. This is consistent with our observations on the components of air velocity. As stated earlier, since the walks are in the opposite directions, some of the kinetic energy from the moving body would be used to invert the direction of air. That is why walking twice did not precisely double the kinetic energy of air.

4 | CONCLUSIONS AND LIMITATIONS

This study aims to characterize the effect of human movement on airflow patterns by high-resolution and three-dimensional measurements of air velocity in a controlled chamber. As stated in the introduction, researchers have made various attempts on this issue from qualitative approach [25] to computer simulations [29,47] and scaled experiments [34] to surrogate (ie, particles or tracer gas) measurements.[30] However, this work is the first of its kind that measures air velocities for real human walk. This is, in part, due to employing a state-of-the-art ultrasound indoor air velocity sensor. This technology has put the research team in a unique position of measuring the velocity filed under different initial conditions, for different walking schemes, and using two different set of measurements sensors. Each test was repeated at least 24 times to assure the repeatability and consistency of the experimental outcomes. Access to a limited number of sensors resulted in measurements in the one-foot vicinity of the walking track. Another limitation of this study was that due

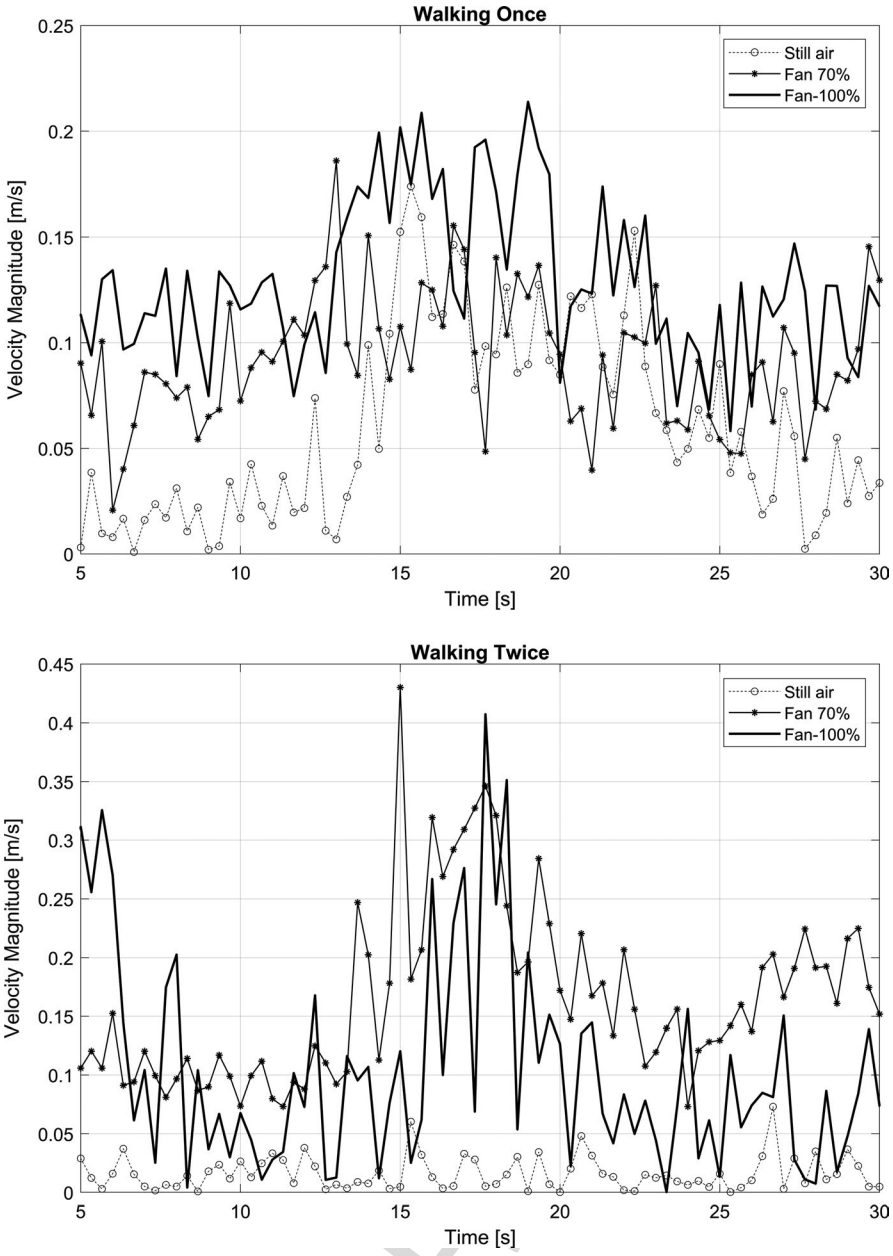

FIGURE 7 Velocity Magnitudes in Sensor L4 for Three Initial Conditions and Two Walking Schemes

to the large number of test and limited time in the chamber we were only able to define a walking twice test of opposite walking directions. Also, at the time of the experiments, the ultrasound sensors had not been commercialized and one could see unreasonable large data logs (>2.0 m/s) due to mixing signals. The research team manually omitted those large data logs during the data analysis phase. These data points occurred in a very few occasions. For instance, a one-minute test with 710 data logs had approximately 15 such data points.

This study indicated that a walking motion with an average speed of 1.02 m/s can have sustained impacts on the magnitude of air velocity as the movement progressed in time. The walking movements generated wakes and carried the wakes with the moving body which was evident from the airflow distribution across the whole region when no predominant inlet airflow was present (ie, still air). Even with inlet airflow, the movement of the individual was able to alter the airflow properties noticeably. As the walk progressed, the wakes carried behind the moving body interacted with the existing flow field, generating turbulence, which resulted in the increase in airflow velocities. Higher values of velocity magnitude were observed up to 1m away from the moving body and were sustained up to 15 seconds after the end of walking. The change in the flow field was realized with a short lag behind the moving object. The first sensors recorded higher airspeeds nearly immediately after the walk commenced. But the last row of sensors had almost 2s lag to realize the human walk. These experiments were conducted under limited conditions, where almost every aspect, starting from walking direction, speed, and directions were controlled. Under the assumed conditions, this study can substantiate that a detectable flow of airstream can sustain up to 10 s in the direction of walk, after the moving body has passed by. Additionally, the walking-induced wake flows will mostly be contained within 1m perpendicular to the principal walking direction,

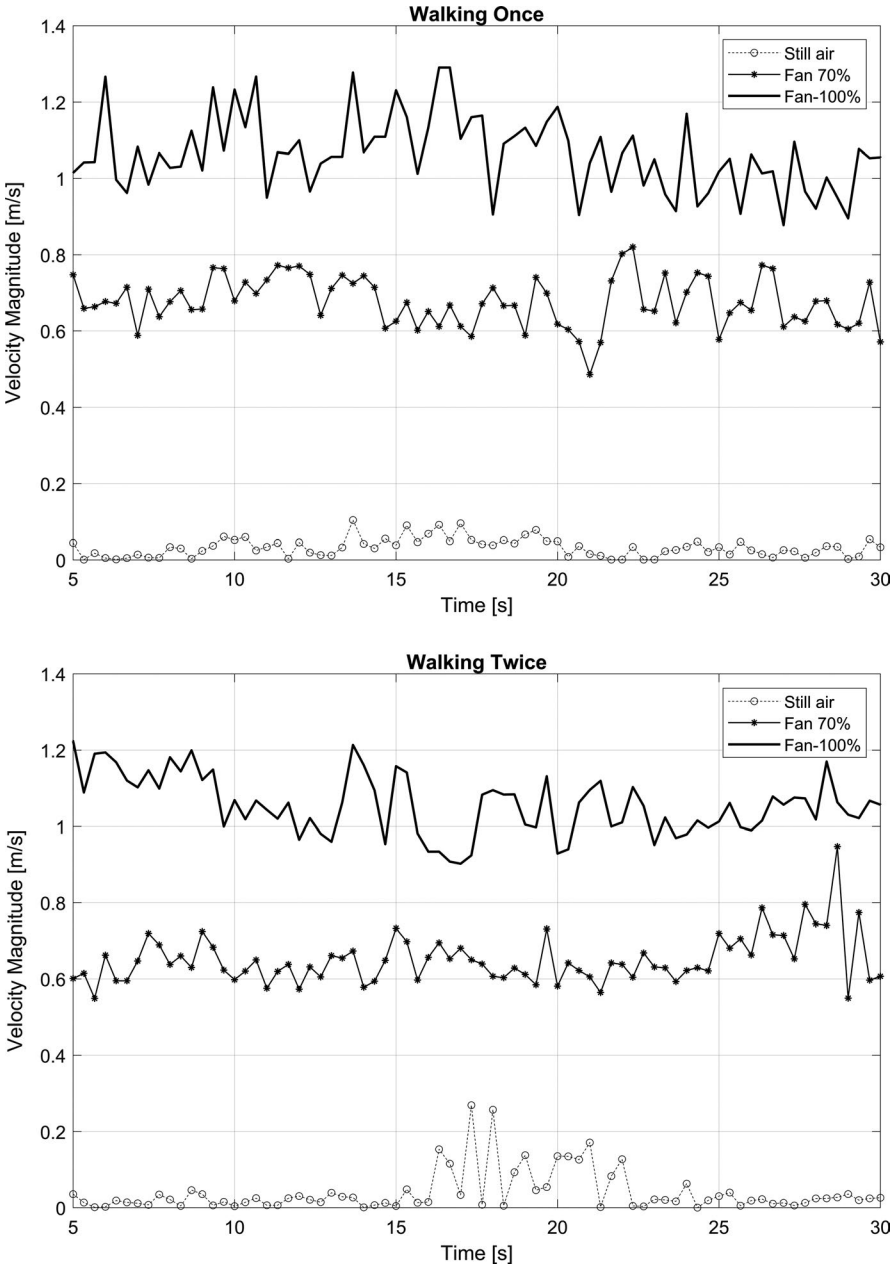

FIGURE 8 Velocity Magnitudes in Sensor R4 for Three Initial Conditions and Two Walking Schemes

TABLE 6 Kinetic Energy of Human Walking vs. Initial Condition

Initial condition	Still Air		70% Fan		100% Fan	
Walking status	Walking Once	Walking Twice	Walking Once	Walking Twice	Walking Once	Walking Twice
K_o	0.012	0.015	1.197	1.123	2.689	2.658
K_W	0.044	0.068	1.255	1.218	2.837	2.888
$\Delta K = K_W - K_o$	0.032	0.053	0.057	0.095	0.148	0.229
ΔK (twice)/ ΔK (once)	1.682		1.651		1.549	

when the walking speed is not drastically different than that of our experiments.

Another significant observation was the behavior of the velocity components due to walking. A dominant unidirectional move along the x-axis resulted in significant values for the y and z velocity components. The z component is claimed to be responsible for the resuspension of settled particulate matters. Furthermore, opposite walking directions reduce the velocity magnitudes along the walking

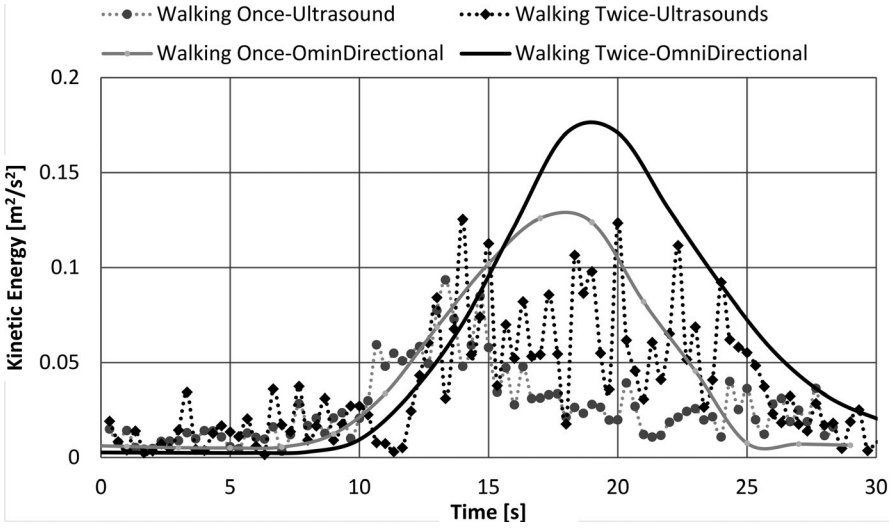

FIGURE 9 Total Kinetic Energy of Still Air for Two Walking Schemes and Two Measurement Techniques; Sum Over All Sensor Locations

track while increasing the velocity normal to the walking track (eg, pushing air to the side). Nonetheless, it seemed that the alterations resulting from the moving body are similar for different walking motions which provides the opportunity of predictability of flow field changes due to human walk. This is an interesting direction to carry forward this research. It is notable that even though the walk performed during tests were realistic human walk, the restricted experimental setup and lack of pertinent instruments, limited our ability to gather and analyze data associated with the swinging arm and leg motions.

This study investigated the kinetic energy of air as it related to human walking. The results consistently showed a raise (ΔK) over the background kinetic energy due to the human walk. ΔK was larger when air inlet performed at full capacity, perhaps due to higher amplitude velocity fluctuations over the mean (ie, turbulence). When ΔK for walking once and walking twice was compared, the increase seemed to be independent of the initial condition. This observation motivates the idea of predicting airflow patterns due to multiple walks from a known walking case. From this study was that strong flow field from high-velocity supply air was able to contain the effects of movement to a very small area; in other words, the effects of walking movement on the flow properties were more prominent in the absence of a dominant air supply. Additionally, it was also demonstrated that further down the direction of the walk, more apparent is the change in airspeed.

ACKNOWLEDGEMENTS

This project is funded by the US National Science Foundation under the Grant Number 2012827. Special thanks to the faculty and staff of the Center of Built Environment (CBE) at the University of California-Berkeley for their assistance with the experiments.

AUTHOR CONTRIBUTION

Arup Bhattacharya: Formal analysis (equal); Methodology (equal); Validation (equal); Visualization (equal); Writing-original draft (lead). **Jovan Pantelic:** Conceptualization (supporting); Methodology (equal); Resources (supporting); Supervision (supporting); Writing-review & editing (equal). **Ali Ghahramani:** Methodology (supporting); Resources (equal); Supervision (supporting); Writing-review & editing (equal). **Ehsan Mousavi:** Conceptualization (lead); Formal analysis (lead); Funding acquisition (lead); Investigation (lead); Methodology (lead); Resources (equal); Supervision (lead); Validation (equal); Visualization (equal); Writing-original draft (equal); Writing-review & editing (lead).

PEER REVIEW

The peer review history for this article is available at https://publons.com/publon/10.1111/ina.12735.

DATA AVAILABILITY STATEMENT

Data are available on request from the authors.

ORCID

Jovan Pantelic https://orcid.org/0000-0001-7541-8274
Ehsan S. Mousavi https://orcid.org/0000-0003-4970-5709

REFERENCES

1. Sundell J. On the history of indoor air quality and health. *Indoor Air*. 2004;14(s7):51-58.
2. Awbi HB. *Ventilation of Buildings*. Taylor and Francis; 2003.
3. Whyte W. *Cleanroom Technology Fundamentals. Testing, and Operation*. John Willey and Sons. 2001.
4. Frienda J, Yeo L. Fabrication of microfluidic devices using polydimethylsiloxane. *Biomicrofluidics*. 2010;4(2):265025.
5. Mousavi E, Betz F, Lautz R. Academic Research to Support Facility Guidelines Institute & ANSI/ASHRAE/ASHE Standard 170–2013. AHA Data & Insight. 2019.
6. Heffernan DS, Evans HL, Huston JM, et al. Surgical Infection Society Guidance for Operative and Peri-Operative Care of Adult Patients Infected by the Severe Acute Respiratory Syndrome Coronavirus-2 (SARS-CoV-2). *Surg Infect (Larchmt)*. 2020;21(4):301-308.
7. Garner JS. Epidemiol HICPACG for isolation precautions in hospitals. ICH, Hospital Infection Control Practices Advisory Committee.

Guideline for isolation precautions in hospitals. *Infect Control Hosp Epidemiol*. 1996;17:53-80.
8. Hathway A, Papakonstantis I, Bruce-Konuah A, Brevis W. Experimental and modelling investigations of air exchange and infection transfer due to hinged-door motion in office and hospital settings. *Int J Vent*. 2015;14(2):127-140.
9. Hu SC, Wu YY, Liu CJ. Measurements of air flow characteristics in a full-scale clean room. *Build Environ*. 1996;31(2):119-128.
10. Khalil EE.Thermal Management in Healthcare Facilities: Computational Approach. In: Aerospace Sciences Meeting Including The New Horizons Forum and Aerospace Exposition 5. 2009:1–8.
11. Mousavi ES, Grosskopf KR. Secondary exposure risks to patients in an airborne isolation room: Implications for anteroom design. *Build Environ*. 2016;104:131-137.
12. Chung KC, Hsu SP. Effect of ventilation pattern on room air and contaminant distribution. *Build Environ*. 2001;36(9):989-998.
13. Zhou B, Ding L, Li F, Xue K, Nielsen PV, Xu Y. Influence of opening and closing process of sliding door on interface airflow characteristic in operating room. *Build Environ*. 2018;144:459-473.
14. ASHRAE Standard 170. Ventilation of Health Care Facilities. 2013.
15. Liu JY, Wu YH, Cai M, Zhou CL. Point-prevalence survey of healthcare-associated infections in Beijing, China: A survey and analysis in 2014. *J Hosp Infect*. 2016;93(3):271-279.
16. Xie D-S, Xiong W, Xiang L-L, et al. Point prevalence surveys of healthcare-associated infection in 13 hospitals in Hubei Province, China, 2007–2008. *J Hosp Infect*. 2010;76(2):150-155.
17. Gustafson TL, Lavely GB, Brawner ER, Hutcheson RH, Wright PF, Schaffner W. An outbreak of airborne nosocomial varicella. *Pediatrics*. 1982;70:550-556.
18. Josephson A, Gombert ME. Airborne transmission of nosocomial varicella from localized zoster. *J Infect Dis*. 1988;158(1):238-241.
19. Li Y, Leung GM, Tang JW, et al. Role of ventilation in airborne transmission of infectious agents in the built environment - A multidisciplinary systematic review. *Indoor Air*. 2007;17(1):2-18.
20. Beggs CB, Kerr KG, Noakes CJ, Hathway EA, Sleigh PA. The ventilation of multiple-bed hospital wards: Review and analysis. *Am J Infect Control*. 2008;36(4):250-259.
21. Eames I, Shoaib D, Klettner CA, Taban V. Movement of airborne contaminants in a hospital isolation room. *J R Soc Interface*. 2009;6(suppl 6):S757-S766.
22. Leclair JM, Zaia JA, Levin MJ, Congdon RG, Goldman DA. Airborne transmission of chickenpox in hospital. *N Engl J Med*. 1980;302(8):450-453.
23. Shih YC, Chiu CC, Wang O. Dynamic airflow simulation within an isolation room. *Build Environ*. 2007;42(9):3194-3209.
24. Hang J, Li Y, Ching WH, et al. Potential airborne transmission between two isolation cubicles through a shared anteroom. *Build Environ*. 2015;89:264-278.
25. Mattsson M, Sandberg M. Velocity Field Created by Moving Objects in Room. In: *Proc. Of the 5th International Conference on Air Distribution in Rooms*. 1996:547-554.
26. Bjorn E, Mattsson M, Sandberg M, Nielson V. Displacement Ventilation – Effects of Movement and Exhalation. In: Proc. Of Healthy Buildings. 1997:163–168.
27. Nielsen PV. The importance of thermal manikins as a source and obstacle in full-scale experiments. In: *Proceedings of the 3rd International Meeting on Thermal Manikin Testing 3IMM*, Stockholm, Sweden. 1999.
28. Poussou SB, Mazumdar S, Plesniak MW, Sojka PE, Chen Q. Flow and contaminant transport in an airliner cabin induced by a moving body: Model experiments and CFD predictions. *Atmos Environ*. 2010;44(24):2830-2839.
29. Luo N, Weng W, Xu X, Fu M. Human-walking-induced wake flow – PIV experiments and CFD simulations. *Indoor Built Environ*. 2018;27(8):1069-1084.
30. Mazumdar S, Yin Y, Guity A, Marmion P, Gulick B, Chen Q. Impact of moving objects on contaminant concentration distributions in an inpatient ward with displacement ventilation. *HVAC R Res*. 2010;16(5):545-563.
31. Brohus H, Balling KD, Jeppesen D. Influence of movements on contaminant transport in an operating room. *Indoor Air*. 2006;16(5):356-372.
32. Han ZY, Weng WG, Huang QY, Fu M, Yang J, Luo N. Aerodynamic characteristics of human movement behaviours in full-scale environment: Comparison of limbs pendulum and body motion. *Indoor Built Environ*. 2015;24(1):87-100.
33. Wu Y, Gao N. The dynamics of the body motion induced wake flow and its effects on the contaminant dispersion. *Build Environ*. 2014;82:63-74.
34. Rouaud O, Havet M, Solliec C. Influence of external perturbations on a minienvironment: Experimental investigations. *Build Environ*. 2004;39(7):863-872.
35. Cheng Y, Lin Z. Experimental investigation into the interaction between the human body and room airflow and its effect on thermal comfort under stratum ventilation. *Indoor Air*. 2016;26(2):274-285.
36. Matsumoto H, Ohba Y. The influence of a moving object on air distribution in displacement ventilated rooms. *J Asian Archit Build Eng*. 2004;3(1):71-75.
37. Choi JI, Edwards JR. Large-eddy simulation of human-induced contaminant transport in room compartments. *Indoor Air*. 2012;22(1):77-87.
38. Han Z, Sze To GN, Fu SC, Chao CYH, Weng W, Huang Q. Effect of human movement on airborne disease transmission in an airplane cabin: Study using numerical modeling and quantitative risk analysis. *BMC Infect Dis*. 2014;14(1):1-19.
39. Tao Y, Inthavong K, Tu J. Computational fluid dynamics study of human-induced wake and particle dispersion in indoor environment. *Indoor Built Environ*. 2017;26(2):185-198.
40. Bhattacharya A, Metcalf AR, Nafchi AM, Mousavi ES. Particle dispersion in a cleanroom – effects of pressurization, door opening and traffic flow. *Build Res Inf*. 2020;1-14.
41. Saidi MH, Sajadi B, Molaeimanesh GR. The effect of source motion on contaminant distribution in the cleanrooms. *Energy Build*. 2011;43(4):966-970.
42. Hang J, Li Y, Jin R. The influence of human walking on the flow and airborne transmission in a six-bed isolation room: Tracer gas simulation. *Build Environ*. 2014;77:119-134.
43. Bauman FS, Arens EA, Tanabe S, Zhang H, Baharlo A. Testing and optimizing the performance of a floor-based task conditioning system. *Energy Build*. 1995;22(3):173-186.
44. Ghahramani A, Zhu M, Przybyla RJ, et al. Measuring Air Speed with a Low-Power MEMS Ultrasonic Anemometer via Adaptive Phase Tracking. *IEEE Sens J*. 2019;19(18):8136-8145.
45. Arens E, Ghahramani A, Przybyla R, et al. Measuring 3D indoor air velocity via an inexpensive low-power ultrasonic anemometer. *Energy Build*. 2020;211:109805.
46. Ghahramani A, Zhu M, Przybyla R, et al. An Inexpensive Low-Power Ultrasonic 3-Dimensional Air Velocity Sensor. *Proc IEEE Sensors*. 2019;11-14.
47. Chen C, Lin CH, Wei D, Chen Q. Modeling particle deposition on the surfaces around a multi-slot diffuser. *Build Environ*. 2016;107:79-89.

How to cite this article: Bhattacharya A, Pantelic J, Ghahramani A, Mousavi ES. Three-dimensional analysis of the effect of human movement on indoor airflow patterns. *Indoor Air*. 2020;00:1–15. https://doi.org/10.1111/ina.12735